Measurement of Attenuation and Speed of Sound in Soils

Michael L. Oelze, William D. O'Brien, Jr., and Robert G. Darmody*

ABSTRACT

The potential application of this work is the detection and imaging of buried objects using acoustic methodology. To image buried artifacts, it is vital to know speed and attenuation of sound in the particular soil being examined because they vary in different soil types and at different moisture contents. To that end, our research involved six soils representing a range of properties expected to influence acoustic response. Clay ranged from 2 to 38%, silt from 1 to 82%, sand from 2 to 97%, and organic matter from 0.1 to 11.7%. Signals from an acoustic source were passed through soil samples and detected by an acoustically coupled hydrophone. From a total of 231 evaluations, we determined the acoustic attenuation coefficient and the propagation speed of sound in the soil samples as a function of four levels of soil moisture and two levels of compaction. Attenuation coefficients determined over frequencies of 2 to 6 kHz ranged from 0.12 to 0.96 dB cm^{-1} kHz^{-1}. Lower attenuation tended to be in loose dry samples. Correlation coefficients were 0.35 (P = 0.01) and 0.31 (P = 0.03) between attenuation and soil water content and soil bulk density, respectively. Propagation speeds ranged from 86 to 260 m s^{-1}. The correlation coefficient with speed was −0.28 (P = 0.05) for soil water content and −0.42 (P = 0.002) for total porosity. Given the acoustic properties, it is theoretically possible to detect an object down to ~40 cm below the soil surface.

Locating buried artifacts is a concern to large landowners such as the defense department because they are required to protect archaeological and cultural sites in their vast landholdings. Once a cultural or archaeological resource site is identified, it must then be assessed to determine its significance and eligibility for National Registry of Historic Places (Executive Order 11593). A Phase II eligibility assessment currently costs about $10 000 to $30 000 per site. Given that there are ~120 000 archaeological sites in the U.S. Army alone, the cost of complete Phase II assessments is prohibitive. Therefore, there is an urgent need to significantly reduce the cost of data recovery at sites with an unknown probability of containing significant cultural or archaeological resources. A method that would detect buried artifacts from the surface would avoid the expense and complications that excavation causes. We propose an acoustic system that could detect and classify buried artifacts (Frazier et al., 2000). As a necessary prelude to the development of such a system, basic acoustic properties for the production, detection, and processing of acoustic signals in soils need to be determined.

Before an acoustic imaging system can be designed, an understanding of basic properties of acoustic propagation in various soils and in different soil conditions is required. These basic properties of the soil can then be evaluated to assess the acoustic imaging tradeoffs for detecting and characterizing buried artifacts. The acoustic attenuation coefficient is used to assess the tradeoff between imaging depth and resolution. The acoustic propagation speed is used to assess resolution and to evaluate the acoustic impedance for transducer design considerations.

Acoustic wave propagation has been utilized to image and characterize properties of different porous materials. Ultrasonic waves have been used to image and characterize living tissues. Seismic waves of frequency below 100 Hz have been used to explore deep into the earth. The choice of acoustic frequency depends on the particular media being examined. To obtain significant resolution of objects at depths less than a meter in soils, acoustic frequencies on the order of 0.5 to 6 kHz should be used.

The behavior of sound propagation in porous media is described by the Biot theory (Biot, 1956a,b), which predicts the propagation of two compressional waves and a shear wave in a porous medium. The existence of these waves in a porous material was confirmed in the experiments of Plona (1980). The first compressional wave is characterized by particle motion in phase with the fluid motion. The second compressional wave is characterized by particle motion out of phase with the fluid motion. The first wave is often referred to as the fast compressional wave because it generally has a higher speed than the wave of the second type, or slow compressional wave. Also, the slow compressional wave generally has a much higher attenuation than the fast compressional wave. The shear wave has the slowest speed and greatest attenuation.

Saturation levels in a porous material have been shown to affect the speed and attenuation of compressional and shear waves (Tittmann et al., 1980; Velea et al., 2000). The slow wave is difficult to observe in sediments or soils saturated with water because of the high attenuation and the way in which the sound is coupled at the soil or sediment interface (Stoll and Kan, 1981). Claims of observing the propagation of a slow wave in sediments have been made by Chitiros (1995). Recent studies by Thorsos et al. (2000) have indicated that the supposed slow wave measurements by Chitiros may actually be because of scattering from roughness at the water-sediment interface. Whether or not the slow wave can be measured in sediments is still questionable, however, if the slow wave does exist in water-saturated soils or sediments its effect is small.

As the fluid in the pore space becomes less viscous,

M.L. Oelze and W.D. O'Brien, Jr., Dep. of Electrical and Computer Engineering, Univ. of Illinois, Urbana, IL 61801; and R.G. Darmody, Dep. of Natural Resources and Environmental Sciences, Univ. of Illinois, 1102 S. Goodwin Ave., Urbana, IL 61801. Received 4 Jan. 2001. *Corresponding author (rdarmody@uiuc.edu).

Published in Soil Sci. Soc. Am. J. 66:788–796 (2002).

Abbreviations: ADA, Adrian soil; CAB, Catlin soil; COLE, coefficient of linear extensibility; DRA, Drummer soil; MEA, Medway soil; NRL, Naval Research Laboratory; PLA, Plainfield soil; SAC, Sable soil; TOF, time of flight.

Table 1. Locations and classifications of soils sampled for acoustic characterization.

Soil Code	Soil series	Soil classification	Soil horizon	Sample depth	Latitude	Longitude
				cm	° ′ ″	
ADA	Adrian	sandy or sandy-skeletal mixed, euic, mesic Terric Haplosaprists	A	0–20	40 01 00	90 24 00
CAB	Catlin	fine-silty, mixed, superactive mesic, Oxyaquic Argiudolls	Bt	73–85	40 05 14	88 13 55
DRA	Drummer	fine-silty, mixed, superactive, mesic, Typic Endoaquolls	Ap	0–20	40 05 01	88 13 55
MEA	Medway	fine-loamy, mixed, superactive, mesic, Fluvaquentic Hapludolls	Ap	0–20	40 00 00	90 28 00
PLA	Plainfield	mixed, mesic Typic Udipsamment	Ap	0–20	40 09 28	90 05 14
SAC	Sable	fine-silty, mixed, superactive mesic, Typic Endoaquolls	Cg	300–320	40 00 00	88 42 30

the observation of slow wave propagation becomes more likely (Bourbié et al., 1987). Measurements of the slow wave have been made for air-soil interfaces (Sabatier et al., 1986). In the rigid-frame limit of Biot theory (Geertsma and Smit, 1961; Attenborough, 1987) the two compressional waves reduce to a single wave, the slow wave. Analyses of the rigid-frame limit have allowed the deduction of pore properties of soils such as the total porosity, tortuosity, and permeability from measurements of the slow wave in air-filled soils (Attenborough, 1983; Sabatier et al., 1990; Moore and Attenborough, 1992). The measurement techniques used to deduce pore properties were the level difference technique and a probe microphone technique (Sabatier et al., 1996). In these measurement techniques, sound is incident on a porous surface through the air and is coupled mainly to the air in the pores producing the slow wave. Typically, the slow wave penetrates the soil down to only a few centimeters because of its high attenuation and dispersion.

The slow wave can be used to image artifacts in soils up to a few centimeters (Sabatier et al., 1998), but would not propagate far enough to image objects buried deeper. To image artifacts that are buried deeper than a few centimeters, acoustic energy should be coupled more to the frame itself. Coupling sound to the frame of the soil would direct more energy to the fast compressional wave that typically has a significantly smaller attenuation than the slow wave. Coupling sound to the frame of the soil can be accomplished with either contact methods (Hickey and Sabatier, 1997) or from sound incident on the soil through a solid or fluid layer with impedance closer to the soil frame (Geertsma and Smit, 1961; Albert, 1993). For this experiment, the latter coupling method was used.

MATERIALS AND METHODS

Acquisition and Evaluation of the Soil Samples

Soil samples were collected to represent a wide range of properties expected to influence acoustic response including organic matter, sand, silt, and clay contents (Table 1). Prior to acoustic characterization, the soil samples were air-dried and sieved to exclude material >2 mm. The influence of vegetative cover, coarse-fragment content, structure, and other features of undisturbed soils in the field were not addressed by this phase of the work. Soil characterization was by standard methodology (Table 2). Particle-size analysis was determined by the hydrometer method for clay and silt, sieves were used for the sand fraction (Gee and Bauder, 1986). Organic C content was determined by wet combustion with sodium dichromate using a conversion factor of 1.724 (Nelson and Sommers, 1986). Liquid and plastic limits and plasticity index were determined with a glass plate and an electric liquid limit machine (American Association of State Highway Officials, 1969). Coefficient of linear extensibility (COLE) was determined by air drying wet samples created with an extrusion device (Schafer and Singer, 1976).

The experimental design included samples from six soils, two compaction levels (loose and compacted), and four moisture levels (air-dried to saturated) for a total of 48 experimental combinations. However, the Plainfield soil (mixed, mesic Typic Udipsamments) was evaluated only loosely compacted at the low-moisture level, and the saturated soil was not compacted, yielding a total of 41 experimental combinations. The acoustic properties were evaluated at a minimum of three soil thicknesses ranging from 5 to 27 cm. The procedure for obtaining a soil thickness involved placing a weighed, measured thickness of soil in a volumetrically calibrated plastic tub (~30 cm high by 30-cm diam.) prior to acoustic evaluation (Fig. 1). A total of 231 frequency-dependent acoustic acquisitions were made.

A small sample of soil was removed to determine gravimetric moisture content immediately after each acoustic evaluation. Water content of the soils was determined by weight loss on drying, volumetric water content was calculated from the bulk density, given the moist volume and calculated dry weight of the sample in the tub (Blake and Hartge, 1986; Gardner, 1986). Total porosity was calculated based on the average soil particle density, estimated by adjusting the inorganic particle density of 2.65 g cm^{-3}, by the soil organic matter content at a density of 1.5 g cm^{-3}, given the total dry weight and volume (Danielson and Sutherland, 1986).

Initial water content of the soils for acoustic evaluation was air-dry. The two next higher water contents were nominally

Table 2. Physical properties of acoustically characterized soil materials.

Soil code†	Sand	Silt	Clay	Organic matter	Soil texture class	Liquid limit	Plastic limit	Plasticity index	COLE
	%								%
ADA	72	18	10	11.7	fine sandy loam	NP‡	NP	NP	NP
CAB	11	53	36	0.5	silty clay loam	43	24	19	14
DRA	12	50	38	9.8	silty clay loam	43	28	15	13
MEA	38	38	24	2.3	loam	28	19	9	7
PLA	97	1	2	0.4	sand	NP	NP	NP	NP
SAC	2	82	16	0.1	silt loam	29	24	5	4

† ADA, Adrian soil, A-horizon; CAB, Catlin soil, Bt-horizon; DRA, Drummer soil, Ap-horizon; MEA, Medway soil, Ap-horizon; PLA, Plainfield soil, Ap-horizon; SAC, Sable soil, Cg-horizon.
‡ NP, non-plastic.

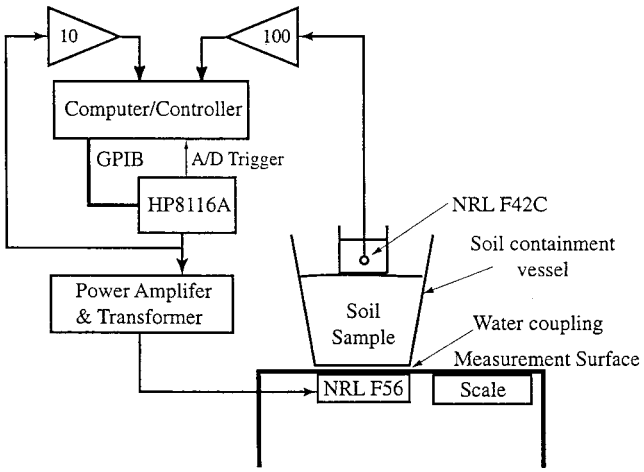

Fig. 1. Block diagram of the soil acoustic characterization system.

increased to 10 and 25% water by volume. This was achieved by carefully adding the appropriate quantity of water and thoroughly mixing and screening the moist soil through a 4-mm sieve. The soil was brought to saturation by adding screened moist soil to standing water. All moist soils were allowed to equilibrate for at least 24 h before acoustic acquisition under cover and at a constant temperature to prevent evaporation.

The loose compaction of the soils was achieved by pouring moisture-adjusted soil through a 4-mm sieve into the calibrated tub and striking off a level surface at the desired thickness. Compaction was achieved by adding a succession of 2-cm lifts to the bottom of the tub. Each lift was compacted with a force applied by a 110-kg mass pressed down on a plywood disk placed on the soil surface. This was repeated until the desired soil thickness was achieved. Compaction, expressed as bulk density on a dry weight basis, was calculated from the total soil weight and volume, using the dry weight back calculated for the computation. The necessary data for this calculation was collected from each sample at the time of its acoustic evaluation, thus compensating for interactions among soil treatments. Obtaining a desired soil thickness by adding layers could lead to heterogeneity in the different soil layers. Thickness layers were also constructed by removing different levels of the compacted soil in the tub. Measurements on soil thickness layers made by adding and removing soil ensured that effects of possible heterogeneities in the layers were minimized and that the experiment was repeatable.

For record keeping purposes, the acoustic data were recorded in files that were named to identify the experimental soil conditions. The first three letters in the file name were the soil code (Table 1). The next two numbers were the sample thickness in centimeters (5- to 27-cm range). The next digit was the moisture code, 1, 2, 3, or 5 for air-dry, nominally 10%, nominally 25%, and saturated, respectively. The next digit was the compaction code, 1 for loose, 4 for compact. The last number in the file name represented the replication of those soil conditions (minimum of two). An additional code was added after the file name to indicate sequence number. Statistical comparisons of soil attributes with sound speed and attenuation were obtained by Pearson Product Moment Correlation, a $P \leq 0.050$ was considered significant (SPSS, 1997).

Acoustic Measurement System and Processing

The soil acoustic characterization system consisted of a host computer, which controlled all data acquisition procedures, and a signal generator, amplifier, and receiver (Fig. 1). A Hewlett Packard HP8116A (with option 001) programmable signal generator (Hewlett-Packard, Palo Alto, CA) received instructions via an IEEE-488 (GPIB) communication bus which produced a low-level signal. A 3000-W power amplifier (Industrial Test Equipment Powertron 3000S, Port Washington, NY) amplified the low-level signal from the HP8116A. The amplifier was impedance matched to the NRL F56 Serial 58 acoustic source (Transducer Branch, U.S. Naval Research Laboratory's [NRL] Underwater Sound Reference Detachment, Orlando, FL) by a transformer (Industrial Test Equipment ET-900V). The overall band width of the power amplifier was between about 10 Hz and 20 kHz.

The acoustic signal was propagated through the soil sample contained in a thin-walled plastic tub coupled to the acoustic source via a water interface. The transmitted acoustic signal was received by a hydrophone (NRL F42C Serial 28, Transducer Branch, U.S. NRL Underwater Sound Reference Detachment, Orlando, FL), which was acoustically coupled to the top of the soil sample with DOW 710 silicon oil (DOW chemical, Midland, MI). The hydrophone was stable and calibrated with a band width between 100 Hz and 200 kHz. The calibration is traceable to the NRL Underwater Sound Reference Detachment.

The low-level signals from the signal generator and from the hydrophone were amplified (custom built high-input impedance operational amplifiers) with gains of 10 and 100, respectively, and the outputs from the amplifiers were digitized. The processing of the acquired data was done off-line in MATLAB (The Math Works, Natick, MA) on a SUNSparc2 workstation (Sun Microsystems, Inc., Palo Alto, CA).

The experimental setup ensured that the coupling of sound would predominantly be apportioned to the soil skeletal frame (type I dilatational wave) as opposed to the fluid in the pores (type II dilatational wave). The impedance mismatch from the water to air is much greater than the water to soil frame. Coupling to the frame would produce fast compressional wave motion whereas coupling to the pore space or air would produce the highly attenuated slow wave. Even with increased saturation of water in the pore space of the soil, the slow wave was not a factor because sound was coupled from a plastic container to the soil frame itself. Any energy that might have been partitioned to the slow wave in the nearly saturated state would be rapidly attenuated.

A list of estimates of the time delay between pulse transmission and reception and records of the amplitude of the received pulse were produced from each single-thickness soil acoustic acquisition. The time estimates were based on the time difference between the received signals from the HP8116A output (the transmitted signal) and the NRL F42C output (the through-transmission received signal). The data were acquired in 250-Hz increments between 1.000 and 10.750 kHz. The estimates were tabulated in 1 kHz increments of frequency, and each value was obtained from four different frequency measurements, i.e., the 1-kHz values were obtained from the scans at 1000, 1250, 1500, and 1750 Hz, from 1 to 10 kHz.

Time of flight (TOF) was estimated by computing the correlation function between the transmitted and received pulses (5-cycles in duration). The frequency-dependent speed of sound estimates were computed by performing linear regressions with respect to soil thickness referenced to the smallest soil thickness. Referencing to the smallest soil thickness allowed the effects of the container and the intermediary fluids to be factored out of speed and attenuation estimates. Speed of sound was calculated as the slope of line that best fits (in a least squares sense) the plot of TOF vs. thickness. Attenuation was determined from the slope of the line that best fit the plot of 20 $\times$ log (received amplitude) vs. thickness. The

20 × log (received amplitude) operation was performed so that attenuation can be reported in dB cm^{-1} kHz^{-1} because the examination of attenuation data yielded a linear dependency with frequency.

Errors to the calculation of attenuation and sound speed were introduced by the limitations of the experimental setup. For the lower frequencies and the smallest layer thickness, the wavelength of sound was on the same order as the layer thickness. Multiple reflections in the layer could add constructively and destructively to the signal received. The processed speed and attenuation measurements were averaged at four frequencies, i.e., 2000, 2250, 2500, and 2750 Hz together for the 2000 Hz signal; these results included reflection and attenuation losses that assisted to minimize errors as the frequency increased because the attenuation losses increased with frequency. Errors resulting from side lobes emitted from the source were nonexistent because the beam pattern was nearly spherical for all frequencies used.

Mass loading by the hydrophone assembly could affect the acoustic propagation factors in the soils, especially near the interface between the hydrophone assembly and the soil. Mass loading increases the stress in the area of soil below the load. Increasing the stress in granular materials will typically increase the propagation speed and decrease the attenuation because the added stress increases the cohesiveness of the granular bonds. The stress applied by the hydrophone assembly because of its weight and area of contact is comparable with the adding of a soil layer for each acoustic measurement. The estimation of acoustic parameters was made using a relative measurement per thickness of soil. The relative measurement scheme would average the overall effects of mass loading by the hydrophone assembly and addition of soil layers. Change in propagation factors with depth and additional stress would amount to increased standard error in the best-fit line versus soil depth. Based on the size of the mean standard deviation for the estimated propagation factors (8% for the propagation speed values, 20% for the attenuation values), the effects of added stress to the soil by mass loading was assumed minimal.

RESULTS

Soil Characteristics

The compaction technique increased the soil bulk densities while decreasing the porosity, although there was some variability within compaction treatments and by soil type (Table 3). With the exception of the wet Sable (SAC 34), Plainfield (PLA) consistently had the highest bulk densities because of its high sand content (Table 2). Adrian (ADA) (sandy or sandy-skeletal, mixed, euic, mesic Terric Haplosaprists) consistently had the lowest bulk densities because of its high organic matter content, which also made it difficult to compact.

At each moisture level, gravimetric soil moisture content varied by soil type. At any given moisture level, Plainfield samples (PLA) tended to have the lowest water content and Adrian (ADA) had the greatest (Table 4). The mean water-filled porosity ranged from 1% for the air-dry Plainfield (PLA) to 99% for the saturated soils (Table 5).

Table 3. Mean bulk density for the six soil sample types by treatment.

Treatment code†	Soil type‡					
	ADA	CAB	DRA	MEA	PLA	SAC
	Bulk density, g cm^{-3}					
11	0.92	1.27	1.32	1.13	1.51	1.36
14	1.03	1.44	1.40	1.37	nd§	1.41
21	0.83	1.16	1.00	1.11	1.45	0.98
24	1.00	1.36	1.19	1.30	1.62	1.36
31	0.79	0.90	0.88	0.97	1.46	1.24
34	0.92	1.14	1.26	1.35	1.57	1.62
51	0.92	1.11	1.27	1.23	1.57	1.35

† The first digit of the code designates soil moisture; 1, air dry, to 5, saturated. The second digit designates soil compaction, 1 is loose and 4 is dense.
‡ ADA, Adrian soil, A-horizon; CAB, Catlin soil, Bt-horizon; DRA, Drummer soil, Ap-horizon; MEA, Medway soil, Ap-horizon; PLA, Plainfield soil, Ap-horizon; SAC, Sable soil, Cg-horizon.
§ nd, not determined.

Table 4. Mean gravimetric water content for the six soil types by treatment.

Treatment code†	Soil type‡					
	ADA	CAB	DRA	MEA	PLA	SAC
	Gravimetric water, %					
11	4.3	3.4	4.4	2.5	0.3	1.8
14	4.3	3.4	4.4	2.3	nd§	1.8
21	15.9	8.6	14.6	10.9	9.1	11.5
24	15.1	8.8	13.7	11.3	8.5	11.6
31	30.6	18.3	28.5	15.7	9.1	22.2
34	30.8	18.6	26.7	16.2	11.1	19.7
51	68.9	52.2	49.0	43.1	26.0	36.4

† The first digit of the code designates soil moisture; 1, air dry, to 5, saturated. The second digit designates soil compaction, 1 is loose and 4 is dense.
‡ ADA, Adrian soil, A-horizon; CAB, Catlin soil, Bt-horizon; DRA, Drummer-soil, Ap-horizon; MEA, Medway soil, Ap-horizon; PLA, Plainfield soil, Ap-horizon; SAC, Sable soil, Cg-horizon.
§ nd, not determined.

Acoustic Evaluations

The soil samples were too acoustically *lossy* (very high attenuation coefficients) to record reliable signals above ~6 kHz; data recorded below 2 kHz were also unreliable. Therefore, all results represent the acoustic frequency range between 2 and 6 kHz. Attenuation coefficients generally increased with compaction and with water content for all but the sandy soils (PLA and ADA) (Table 6). Intuitively, increased compaction, by increasing the number of grain contacts and reducing the loss per contact, should decrease attenuation. Why the increase was observed is not entirely clear and will be the

Table 5. Mean water-filled porosity for the six soil types by treatment.

Treatment code†	Soil type‡					
	ADA	CAB	DRA	MEA	PLA	SAC
	Water-filled pores, %					
11	6.2	8.4	12.1	4.9	1.0	5.2
14	7.5	10.8	14.0	6.7	nd§	5.5
21	19.7	17.8	24.0	20.9	29.0	18.1
24	24.8	24.9	30.9	29.1	35.5	32.2
31	35.0	24.0	38.6	24.0	29.3	51.7
34	44.2	37.6	66.5	45.5	42.6	82.6
51	99.4	99.9	99.4	99.7	99.7	99.9

† The first digit of the code designates soil moisture; 1, air dry, to 5, saturated. The second digit designates soil compaction, 1 is loose and 4 is dense.
‡ ADA, Adrian soil, A-horizon; CAB, Catlin soil, Bt-horizon; DRA, Drummer-soil, Ap-horizon; MEA, Medway soil, Ap-horizon; PLA, Plainfield soil, Ap-horizon; SAC, Sable soil, Cg-horizon.
§ nd, not determined.

Table 6. Mean attenuation coefficient (dB cm^{-1} kHz^{-1}) for the six soil types by treatment. Mean standard deviation is 20% of the reported values.

Treatment code†	Soil type‡					
	ADA	CAB	DRA	MEA	PLA	SAC
	Attenuation coefficient, dB cm^{-1} kHz^{-1}					
11	0.31	0.14	0.21	0.12	0.23	0.39
14	0.20	0.59	0.53	0.63	nd§	0.36
21	0.68	0.36	0.38	0.39	0.35	0.46
24	0.58	0.91	0.56	0.62	0.50	0.69
31	0.39	0.45	0.51	0.28	0.81	0.50
34	0.71	0.90	0.71	0.90	0.16	0.96
51	0.49	0.58	0.58	0.31	0.75	0.38

† The first digit of the code designates soil moisture; 1, air dry, to 5, saturated. The second digit designates soil compaction, 1 is loose and 4 is dense.
‡ ADA, Adrian soil, A-horizon; CAB, Catlin soil, Bt-horizon; DRA, Drummer-soil, Ap-horizon; MEA, Medway soil, Ap-horizon; PLA, Plainfield soil, Ap-horizon; SAC, Sable soil, Cg-horizon.
§ nd, not determined.

Table 7. Mean propagation speed (m s^{-1}) for the six soil types by treatment. Mean standard deviation is 8% of the reported propagation speed values.

Treatment code†	Soil type‡					
	ADA	CAB	DRA	MEA	PLA	SAC
	Propagation speed, m s^{-1}					
11	153	190	177	154	260	140
14	121	150	159	126	nd§	139
21	89	114	118	151	138	117
24	147	102	136	93	103	122
31	87	150	107	161	122	121
34	86	105	245	105	253	176
51	102	102	118	139	189	207

† The first digit of the code designates soil moisture; 1, air dry, to 5, saturated. The second digit designates soil compaction, 1 is loose and 4 is dense.
‡ ADA, Adrian soil, A-horizon; CAB, Catlin soil, Bt-horizon; DRA, Drummer-soil, Ap-horizon; MEA, Medway soil, Ap-horizon; PLA, Plainfield soil, Ap-horizon; SAC, Sable soil, Cg-horizon.
§ nd, not determined.

subject of further investigation. One possible cause may be the effects of layering of damp soil from the compaction process. Future experiments would be concerned with minimizing the existence of strata in the soil from the compaction process.

Propagation speed values ranged between about 100 and 300 m s^{-1} (Table 7) and dispersion was not observed (Fig. 2 and 3). The highest propagation speeds were generally observed for dry soil with loose compaction.

DISCUSSION

The experimental protocol called for measuring the acoustic properties in relatively homogeneous soil samples. This may suggest that the experimental approach for homogeneous soil preparation was a significant factor that contributed to the relatively narrow range of measured acoustic propagation property values. Further experimentation is needed to determine the effects of soil layering, structure, coarse-fragment content, vegetation cover, and other soil properties found under field conditions, on the ability to image artifacts in the soil.

The attenuation coefficient over the 2 to 6 kHz frequency range varied between a low of ~0.1 dB cm^{-1} kHz^{-1}, which was prevalent for the loose, dry (code 11) samples, and a high close to 1 dB cm^{-1} kHz^{-1}, which was prevalent for the moist, compact (code 34) samples. The roundtrip (from signal to target to receiver) propagation loss (quantitatively described in terms of the at-

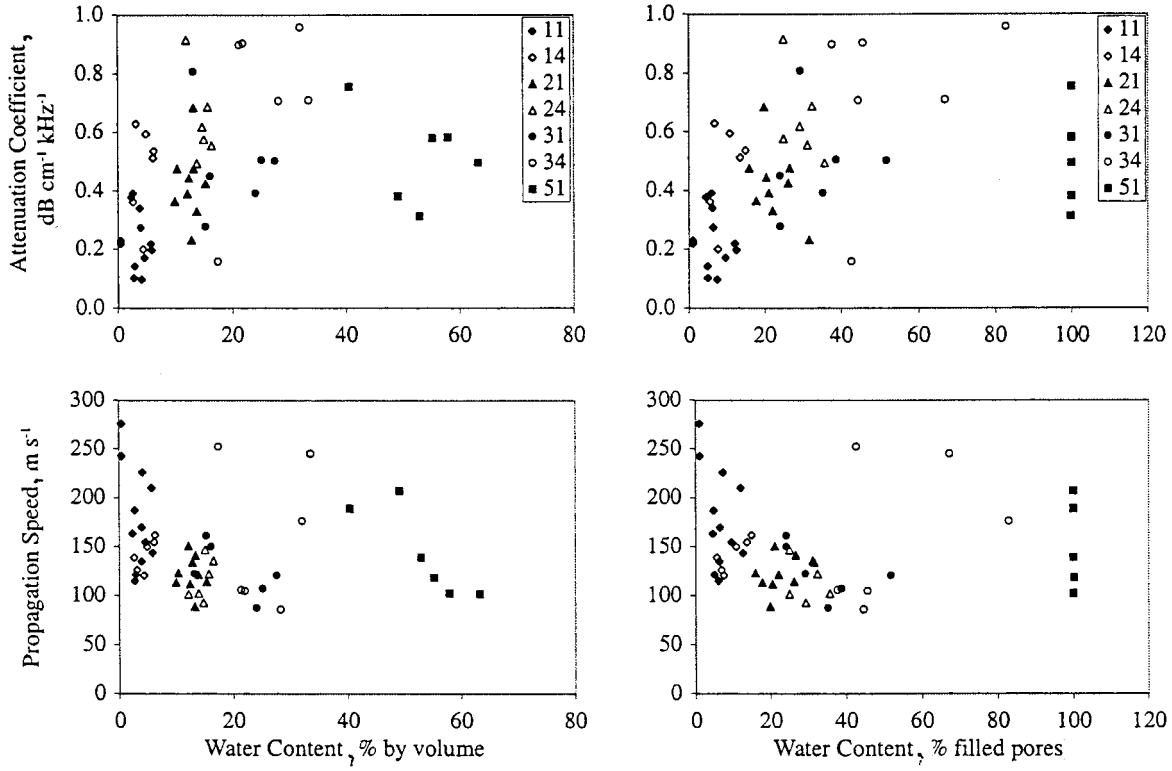

Fig. 2. Attenuation coefficient and propagation speed for all soil samples as a function of water content by volume and by water filled pores.

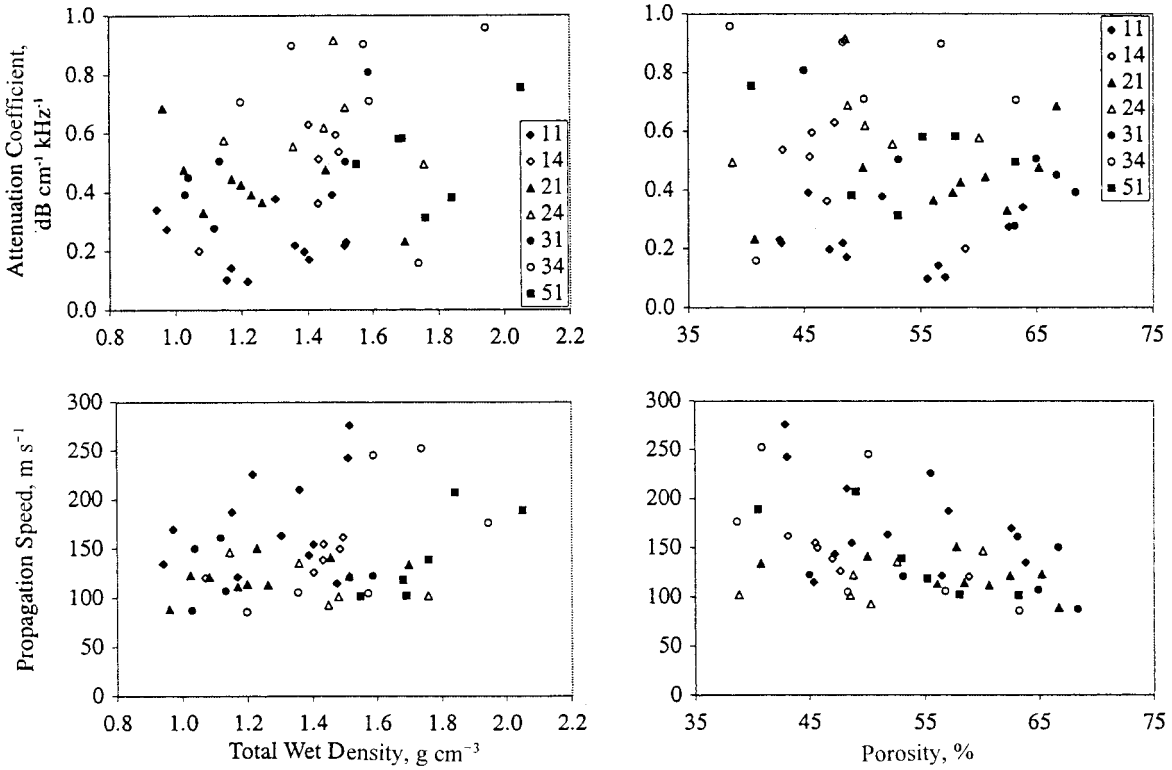

Fig. 3. Attenuation coefficient and propagation speed for all soil samples as a function of total wet density and porosity.

tenuation coefficient) has a direct influence over the imaging depth for an imaging system's dynamic range. Dynamic range represents the extremes of received signals that an imaging system can display. The highest received signal amplitude generally originates from targets near the transducer for which there is minimum roundtrip propagation loss. The lowest received signal amplitude generally originates from targets deeper into the attenuating medium for which there is maximum roundtrip propagation loss. For a specific imaging depth, the roundtrip propagation loss increases as a function of both attenuation coefficient and frequency (Fig 4). If the roundtrip propagation loss cannot exceed about 140 dB (typical of many acoustic imaging systems, but unknown for a subsurface acoustic imaging system), then an imaging depth of about 40 cm is achievable. This presumes an attenuation coefficient of 0.3 dB cm^{-1} kHz^{-1} at a frequency of 6 kHz (144 dB at 40 cm) or of 0.8 dB cm^{-1} kHz^{-1} at a frequency of 2 kHz (141 dB at 44 cm). However, there would be a roundtrip propa-

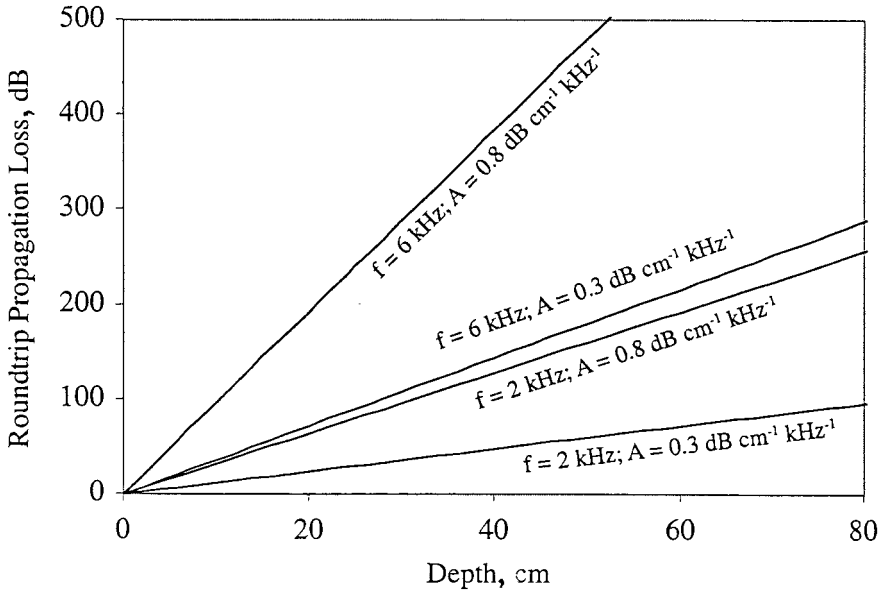

Fig. 4. Example of imaging dynamic range from roundtrip propagation loss (from attenuation) vs. imaging depth as a function of attenuation coefficient and frequency. Reflection coefficient of an object is assumed to be 100%.

Table 8. Correlation coefficients and *P* values ( ) for soil parameters and sound speed and attenuation.

Parameter	Speed/ Attenuation	Water Content (dry basis)	Water Content (wet basis)	Water Content (vol.)	Bulk Density	Water Filled Pores	Porosity
			All Soils				
Speed	−0.39	NS†	−0.28 (0.046)	NS	0.41 (0.003)	NS	−0.42 (0.002)
Attenuation	(0.005)	0.30 (0.034)	0.35 (0.011)	0.36 (0.011)	NS	0.40 (0.004)	NS
			Non-Saturated Soils				
Speed	−0.42	−0.33 (0.026)	−0.35 (0.019)	NS	0.36 (0.014)	NS	−0.37 (0.011)
Attenuation	(0.004)	0.48 (7×10^{-4})	0.50 (0.0004)	0.59 (2×10^{-5})	NS	0.61 (7×10^{-6})	NS
			Saturated Soils				
Speed	NS	−0.84 (0.035)	−0.86 (0.030)	−0.85 (0.032)	0.86 (0.028)	NS	−0.85 (0.031)
Attenuation		NS	NS	NS	NS	NS	NS

† NS, no significant correlations ($P > 0.050$).

gation loss of 384 dB for an imaging depth of 40 cm in a lossy medium at a higher frequency (e.g., attenuation coefficient of 0.8 dB cm^{-1} kHz^{-1} at a frequency of 6 kHz), an unrealistic loss for a typical imaging system's dynamic range.

These dynamic ranges assume that the object is a strong reflector, and virtually the entire reflected echo is directed back to the transducer. Thus, these are best-case dynamic ranges. The acoustic reflection coefficient of the object must also be considered when assessing the overall roundtrip-propagation loss. In general, it appears that the acoustic-reflection coefficient will be ~0 dB based on our results. The characteristic acoustic impedance (product of density and speed) of soil is in the range of (1–3) $\times$ 10^5 Pa s m^{-1} (density ~1000 kg m^{-3}, propagation speed ~100–300 m s^{-1}). A plastic object might have characteristic acoustic impedance in the range of 3.2 $\times$ 10^6 Pa s m^{-1} (for Lucite; density = 1200 kg m^{-3}, propagation speed = 2650 m s^{-1}) whereas a metallic object would have a greater value of characteristic acoustic impedance. The pressure reflection coefficient at normal incidence is:

$$\mathbf{R} = \frac{Z_{\text{object}} - Z_{\text{soil}}}{Z_{\text{object}} + Z_{\text{soil}}} \quad [1]$$

where $Z_{\text{object}} = 3.2 \times 10^6$ Pa s m^{-1} and $Z_{\text{soil}} = 3 \times 10^5$ Pa s m^{-1}, $\mathbf{R} = 0.826$ (or −1.6 dB).

The imaging depth is thus inversely proportional to frequency, which results in the important engineering tradeoff between depth of penetration into soil and image resolution. As a crude rule of thumb, the image resolution can be approximated to that of the acoustic wavelength:

$$\lambda = c\, f^{-1} \quad [2]$$

where c is the propagation speed and f is the acoustic frequency. Thus, as frequency increases the wavelength decreases (resolution improves) and consequently the depth of penetration decreases.

A detailed analysis of the mechanisms responsible for the interaction of the propagated acoustic wave with soil is beyond the scope of this project. However, the initial hypothesis suggested that the acoustic propagation properties of soil might be a function of soil moisture and compaction. Acoustic propagation in granular materials has been explained in terms of contact mechanics (Digby, 1981; Winkler, 1983; Velea et al., 2000). Compaction would have the effect of improving contact between the grains. Saturation in granular materials has been shown to affect the stiffness of contacts between grains (Shields et al., 2000).

A first order examination of the acoustic propagation properties as a function of soil properties (Fig. 2 and 3) do not reveal any obvious trends, except that for the compacted soils attenuation tended to increase with increased water content. There were no significant correlations with liquid or plastic limits, COLE, texture, or organic matter content. However, there were some significant correlations with other soil parameters. For all the soils, speed was negatively correlated with attenuation ($r = -0.39$, $P = 0.005$) (Table 8). The negative correlation between speed and attenuation can be explained by noting that as grain contacts become stiffer the speed increases and the loss between grains becomes less, which results in decreased attenuation.

Similarly, over all soils speed was also negatively correlated with measured water content on a wet weight basis ($r = -0.28$, $P = 0.046$), positively correlated with dry bulk density ($r = 0.41$, $P = 0.003$), and negatively correlated with calculated total porosity ($r = -0.42$, $P = 0.002$). A higher bulk density and decreased porosity through compaction typically indicates greater contact between grains and therefore should produce greater speeds as our data shows. One might expect the speed of sound to approach that of water with increasing saturation, however, preparing a completely saturated sample is difficult (Shields et al., 2000). Several experiments have shown (Brandt, 1960; Domenico, 1976; Anderson and Hampton, 1980) that even small amounts (0.1%) of air will reduce the speed of sound to that below air. Along with being negatively correlated with speed over all soils, attenuation was correlated with volumetric water content ($r = 0.36$, $P = 0.011$) and with water-filled porosity ($r = 0.40$, $P = 0.004$), but was not related to density.

Saturated soils tended to behave differently; there were no significant correlations between attenuation and any soil parameter. Speed in saturated soils tended to increase with bulk density ($r = 0.86$, $P = 0.028$) and decrease with water content ($r = -0.86$, $P = 0.030$). The most significant correlations for attenuation were found in the unsaturated soils. Water-filled porosity ($r = 0.61$, $P = 7 \times 10^{-6}$) and volumetric water content ($r = 0.59$, $P = 2 \times 10^{-5}$) were both strongly correlated with attenuation in unsaturated soils. The increase in attenuation of the acoustic signal occurs because of the viscous

Table 9. Significant correlations between individual soils and sound speed and attenuation.

	Speed		Attenuation	
Soil†	All Treatments	Unsaturated Only	All Treatments	Unsaturated Only
ADA	NS‡	NS	NS	NS
CAB	− attenuation	− attenuation	− speed	− speed, + wpore
DRA	NS	NS	NS	+ wpore, + wvol
MEA	− attenuation	NS	− speed, − pore, + den	− pore, + den
PLA	NS	NS	NS	NS
SAC	+ wpore	NS	NS	+ wpore, + wvol

† ADA, Adrian soil, A-horizon; CAB, Catlin soil, Bt-horizon; DRA, Drummer-soil, Ap-horizon; MEA, Medway soil, Ap-horizon, PLA, Plainfield soil, Ap-horizon; SAC, Sable soil, Cg-horizon.

‡ NS, no significant correlations ($P > 0.050$); + positive correlation; − negative correlation; den, bulk density; pore, porosity; wpore, water-filled porosity; wvol, volumetric-water content.

losses caused by the increase of water in the pore space of the soil.

Individual soils were not too variable in their acoustic properties, which indicate that soil-specific design of the equipment is not a concern. Adrian and PLA soils, the two sandy soils studied, showed no significant correlations between moisture or density and acoustic properties (Table 9). The only significant correlations between speed and attenuation were found in all the treatments of the Catlin (CAB) (fine-silty, mixed, superactive, mesic Oxyaquic Argiudolls) samples and in the unsaturated treatments of the Medway (MEA)(fine-loamy, mixed, superactive, mesic Fluvaquentic Hapludolls) samples. Water-filled porosity was positively correlated with speed in Sable (SAC) (fine-silty, mixed, superactive, mesic Typic Endoaquolls) over all treatments, which goes against the overall trend (Table 9). Correlations between attenuation and individual soils were stronger than with speed. Unsaturated CAB, Drummer (DRA) (fine-silty, mixed, superactive, mesic Typic Endoaquolls), and SAC were positively correlated with water-filled porosity. Attenuation increased with density in MEA soils, and also increased with water content in unsaturated DRA and SAC (Table 9).

In summary, a basic database of acoustic propagation in soil, attenuation coefficient, and propagation speed was developed. This information is crucial in the design of an acoustic image formation system. To obtain an approximate image resolution (see Eq. [2]) of 5 cm, an operating frequency range of 1.7 to 5.2 kHz would be necessary (speed range: 86–260 m s^{-1}). Within this frequency range, an image depth of 30 to 40 cm is feasible for the soils evaluated. These observations have been employed in the design of an acoustic imaging system for soils currently under development (Frazier et al., 2000).

ACKNOWLEDGMENTS

This work was supported by Contract Number DACA88-94-D-0008, U.S. Army Construction Engineering Research Laboratory, Champaign, IL. We thank Tim Ellsworth for his technical review, Nadine Smith and Richard Czerwinski for developing the data acquisition and analysis hardware and software, Dudley Swiney for analyzing the acoustic data, and Scott Wiesbrook, David Tungate, Dan O'Brien, Brett Boege, and Kay Raum for assistance with acoustic data acquisition.

REFERENCES

AASHO. 1969. Standard method for determining liquid limit of soils (T 89-60). Soils Manual, Asphalt Institute. College Park, MD.

Albert, D.G. 1993. A comparison between wave propagation in water-saturated and air-saturated porous materials. J. Appl. Phys. 73:28–36.

Anderson, A.L., and L.D. Hampton. 1980. Acoustics of gas-bearing sediments I. Background. J. Acoust. Soc. Am. 67:1865–1889.

Attenborough, K. 1983. Acoustical characteristics of rigid fibrous absorbent and granular materials. J. Acoust. Soc. Am. 73:785–799.

Attenborough, K. 1987. On the acoustic slow wave in air-filled granular media. J. Acoust. Soc. Am. 81:93–102.

Biot, M.A. 1956a. Theory of propagation of elastic waves in a fluid saturated porous solid. I. Low-frequency range. J. Acoust. Soc. Am. 28:168–178.

Biot, M.A. 1956b. Theory of propagation of elastic waves in a fluid saturated porous solid. II. High-frequency range. J. Acoust. Soc. Am. 28:179–191.

Blake, G.R., and K.H. Hartge. 1986. Bulk density. p. 363–376. *In* A. Klute (ed.) Methods of soil analysis. Part 1. 2nd ed. Agron. Monogr. 9. ASA and SSSA, Madison, WI.

Bourbié, T., O. Coussy, and B. Zinszner. 1987. Acoustics of porous media. Gulf Publishing Co., Éditions Technip, Paris.

Brandt, H. 1960. Factors affecting compressional wave velocity in unconsolidated marine sediments. J. Acoust. Soc. Am. 32:171–179.

Chitiros, N.P. 1995. Biot model of sound propagation in water-saturated sand. J. Acoust. Soc. Am. 97:109–214.

Danielson, R.E., and P.L. Sutherland. 1986. Porosity. p. 443–462. *In* A. Klute (ed.) Methods of soil analysis. Part 1. 2nd ed. Agron. Monogr. 9. ASA and SSSA, Madison, WI.

Digby, P.J. 1981. The effective elastic moduli of porous granular rocks. J. Appl. Mech. 48:803–808.

Domenico, S.N. 1976. Effects of brine-gas mixture on velocity in an unconsolidated sand reservoir. Geophysics 41:882–894.

Frazier, C.H., N. Çadalli, D.C. Munson, Jr., and W.D. O'Brien, Jr. 2000. Acoustic imaging of objects buried in soil. J. Acoust. Soc. Am. 108:147–156.

Gardner, W.H. 1986. Water content. p. 493–544. *In* A. Klute (ed.) Methods of soil analysis. Part 1. 2nd ed. Agron. Monogr. 9. ASA and SSSA, Madison, WI.

Gee, G.W., and J.W. Bauder. 1986. Particle-size analysis. p. 383–412. *In* A. Klute (ed.) Methods of soil analysis. Part 1. 2nd ed. Agron. Monogr. 9. ASA and SSSA, Madison, WI.

Geertsma, J., and D.C. Smit. 1961. Some aspects of elastic wave propagation in fluid-saturated porous solids. Geophysics 26:169–181.

Hickey C.J., and J.M Sabatier. 1997. Measurements of two types of dilatational waves in an air-filled unconsolidated sand. J. Acoust. Soc. Am. 102:128–136.

Moore, H.M., and K. Attenborough. 1992. Acoustic determination of air-filled porosity and relative air permeability of soils. J. Soil Sci. 43:211–228.

Nelson, D.W., and L.E. Sommers. 1986. Total carbon, organic carbon, and organic matter. p. 539–580. *In* A.L. Page et al. (ed.) Methods of soil analysis. Part 2. 2nd ed. Agron. Monogr. 9. ASA and SSSA, Madison, WI.

Plona, T. 1980. Observation of a second bulk compressional wave in a porous medium at ultrasonic frequencies. Appl. Phys. Lett. 36: 259–261.

Sabatier, J.M., H.E. Bass, L.N. Bolen, K. Attenborugh, and V.V.S.S. Sastry. 1986. The interaction of airborne sound with the porous ground: The theoretical formulation. J. Acoust. Soc. Am. 79:1345–1352.

Sabatier, J.M., H. Hess, W.P. Arnott, K. Attenborough, M.J.M. Römkens, and E.H. Grissinger. 1990. In situ measurements of soil physical properties by acoustic techniques. Soil Sci. Soc. Am. J. 54:658–672.

Sabatier, J.M., D.C. Sokol, C.K. Frederickson, M.J.M. Römkens, E.H. Grissinger, and J.C. Shipps. 1996. Probe microphone instrumentation for determining soil physical properties: testing in model porous materials. Soil Tech. 8:259–274.

Sabatier, J.M., X. Ning, and R. Craig. 1998. High-resolution velocity images of targets buried in soils. J. Acoust. Soc. Am. 104:1783.

Schafer, W.M., and M.J. Singer. 1976. A new method of measuring shrink-swell potential using soil paste. Soil Sci. Soc. Am. J. 40:805–806.

Shields, F.D., J.M. Sabatier, and M. Wang. 2000. The effect of moisture on compressional and shear wave speeds in unconsolidated granular material. J. Acoust. Soc. Am. 108:1998–2004.

SPSS. 1997. Sigma Stat version 2.03. SPSS Science, Chicago IL.

Stoll, R.D., and T.K. Kan. 1981. Reflection of acoustic waves at a water-sediment interface. J. Acoust. Soc. Am. 70:149–156.

Thorsos, E.I., D.R. Jackson, and K.L. Williams. 2000. Modeling of subcritical penetration into sediments due to interface roughness. J. Acoust. Soc. Am. 107:263–277.

Tittmann, B.R., V.A. Clark, J.M. Richardson, and T.W. Spencer. 1980. Possible mechanism for seismic attenuation in rocks containing small amount of volatiles. J. Geophys. Res. 85:5199–5208.

Velea, D., F.D. Shields, and J.M. Sabatier. 2000. Elastic wave velocities in partially saturated Ottawa sand: Experimental results and modeling. Soil Sci. Soc. Am. J. 64:1226–1234.

Winkler, K.W. 1983. Contact stiffness in granular porous materials: comparison between theory and experiment. Geophys. Res. Lett. 10:1073–1076.